

Coherent coupling of YBCO superconducting resonators and 100-nm-thick YIG films

Alberto Ghirri^a, Mattia Cavani^b, Claudio Bonizzoni^{b,a}, Marco Affronte^{b,a}

^a*Istituto Nanoscienze - CNR, Centro S3, via G. Campi 213/A, Modena, 41125, Italy*

^b*Dipartimento di Scienze Fisiche, Informatiche e Matematiche, Universita di Modena e Reggio Emilia, via G. Campi 213/A, Modena, 41125, Italy*

Abstract

In cavity magnonics, magnon-photon hybridization has been widely investigated for both fundamental studies and applications. Planar superconducting resonators operating at microwave frequencies have demonstrated the possibility to achieve high couplings with magnons by exploiting the confinement of the microwave field in a reduced volume. Here we report a study of the coupling of high- T_c YBCO superconducting waveguides with 100-nm-thick YIG magnetic films. We study the evolution of mode frequencies at different temperatures and extract the coupling strength of hybrid magnon-photon modes. We show that the experimental results can be reproduced using a simple model in which the temperature dependence of the penetration depth accounts for the evolution of the polaritonic spectrum.

Keywords: Magnons, Spin waves, Microwaves, Strong coupling, Hybrid systems, Superconducting resonators

1. Introduction

Magnon-photon hybrids are obtained by coherently coupling collective excitations in coupled spin systems, that is spin waves and their quantized counterpart magnons, with microwave photon modes. These systems have proven to be fertile ground for both fundamental studies and applications. In the former case, topics like quantum magnonics [1, 2], nonlinear effects [3, 4, 5], ultrastrong coupling [6, 7, 8], non-Hermitian physics [9, 10], Floquet

Email address: alberto.ghirri@nano.cnr.it (Alberto Ghirri)

engineering [11], magnonic frequency combs [12] have been recently investigated. Applications in magnonics and quantum technologies, either at room temperature or in the quantum regime at mK temperatures, are related, but not restricted, to computation, sensing, microwave-to-optical transduction, coherent coupling of remote physical systems, emission of microwaves, among others [13, 14, 15, 16, 17].

For these studies, magnetic materials such as electrically insulating yttrium iron garnet (YIG) or conducting permalloy, which are characterized by high spin densities and low ferromagnetic resonance (FMR) damping rates, have found widespread attention [18]. The incorporation of these materials into superconducting circuits has opened additional possibilities [19, 20, 21, 22]. Microwave modes in planar superconducting resonators have been exploited to achieve strong [23, 24, 25, 26] and ultrastrong [27, 28, 29, 8, 30] coupling with magnons, also using nanomagnets fabricated directly onto the resonator [25, 26]. Furthermore, superconducting qubits were coupled to YIG spheres to detect single-magnon excitations [1, 31].

High critical temperature (T_c) superconducting resonators, in particular $\text{YBa}_2\text{Cu}_3\text{O}_7$ (YBCO), show T_c up to about 90 K and resilience in applied magnetic field [32]. Strong and ultrastrong coupling with spin systems have been achieved, respectively, using paramagnetic ensembles [33, 34, 35, 36] and 5- μm -thick YIG films [8, 30]. In the latter case, the evolution of polaritonic modes at temperature below T_c shows a progressive frequency shift of the hybrid magnon-photon mode, which has been attributed to the effect of Meissner currents and correlated with the penetration depth in the superconducting layer [30].

The spectrum of spin-wave excitations in the YIG film and the coupling with the resonator are dependent upon the thickness of the magnetic layer. We have experimentally investigated the interplay between YBCO and 100-nm-thick YIG films. We first study the broadband spectrum of excitations acquired using a YBCO coplanar waveguide (CPW) transmission line at different temperatures. We then analyze the coupling between microwave and magnon modes using a CPW resonator. We finally discuss how the extracted physical quantities evolve by varying the thickness of the YIG film.

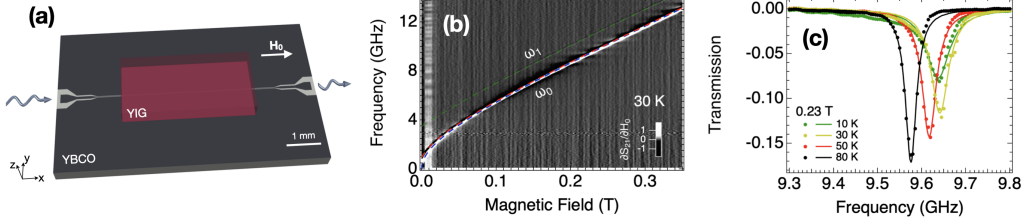


Figure 1: (a) Sketch of the experimental geometry. (b) Spectral map showing the numerical derivative of broadband transmission spectra acquired at $T = 30$ K. Red and green dashed lines show ω_0 and ω_1 as derived respectively from Eq. 2 and Eq 4. The blue dashed line show ω_{FMR} . (c) Evolution, as a function of the temperature, of the S_{21} spectra measured at $\mu_0 H_0 = 0.23$ T. The incident microwave power is -15 dBm. The background transmission, derived from high magnetic field data, was subtracted from the spectra. Solid lines display the Lorentzian fit (Eq. 1).

2. Broadband transmission spectroscopy

We studied a 100-nm-thick YIG film that was grown by liquid phase epitaxy on a 0.5-mm-thick Gadolinium Gallium Garnet (GGG) substrate. The magnetic film was positioned above the YBCO layer and gently pushed from the backside. Transmission (S_{21}) spectra were measured as a function of frequency using a broadband CPW line with the external magnetic field (H_0) applied parallel to the central conductor (Fig. 1(a)). At low temperature ($T = 30$ K), the transmission derivative ($\partial S_{21}/\partial H_0$) map evidences the presence of a main resonance mode at the lowest frequency (ω_0) plus an additional mode (ω_1), which has much weaker amplitude, shifted by approximately 1.2 GHz with respect to the former (Fig. 1(b)).

As a function of frequency, transmission spectra taken at $\mu_0 H_0 = 0.23$ T show well-defined absorption dips (Fig. 1(c)). As the temperature decreases, the resonance frequency, ω_0 , progressively moves toward higher frequencies. The spectral lineshape of the absorption dip, obtained by subtracting the background from the transmission spectra, can be fitted using a Lorentzian curve [37]

$$\bar{S}_{21} = \frac{a}{1 + \left(\frac{\omega - \omega_0}{\frac{1}{2}\Delta\omega}\right)^2}, \quad (1)$$

where ω is the frequency, a is the amplitude and $\Delta\omega$ is the full width at half maximum linewidth (Fig. 1(c)). In particular, from the fits we note that $\Delta\omega$ increases from 30 MHz at 80 K to 64 MHz at 10 K. These values

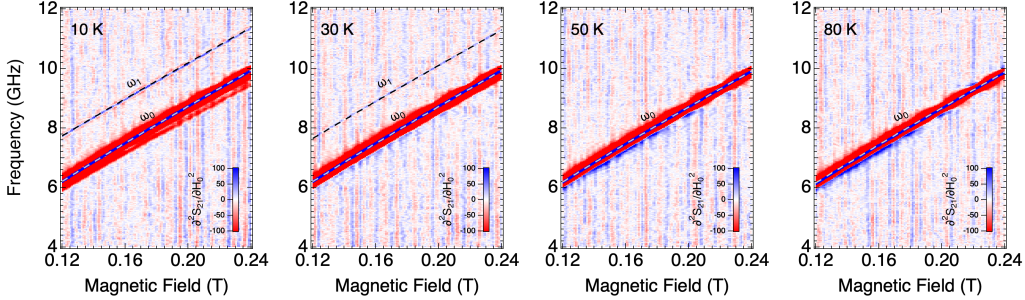


Figure 2: Evolution of broadband spectral maps measured at different temperatures. The color scale shows the second derivative of transmission with respect to the magnetic field. Dashed lines show the curves calculated with Eq. 2 and Eq. 4, as indicated.

are influenced by the presence of both paramagnetic GGG substrate and superconducting YBCO layer as we discuss in the following.

Fig. 2 shows broadband spectral maps taken at temperatures between 80 and 10 K. In order to make the position of the YIG modes more evident, we plot the second derivative of the transmission with respect to the magnetic field $\partial^2 S_{21} / \partial H_0^2$. We note that spectra taken above 50 K show the presence of ω_0 only, while ω_1 is visible at 30 K and below. $\omega_1(H_0)$ curve varies only slightly from 10 K to 30 K (Fig. 2).

Considering the lateral profile of the CPW broadband line and the Damon-Eshbach geometry in our experiment, we expect that the transmission line excites spin wave modes with wavenumber up to $k_y = 3 \times 10^5 \text{ rad m}^{-1} \approx 2\pi/s$ [38, 30]. According to the analytical model by Kalinikos and Slavin (KS) [39], the frequency of the lowest mode can be calculated as [40]

$$\begin{aligned} \omega_0/2\pi &= \\ &= \mu_0 \gamma \sqrt{H_0(H_0 + M_s) + (M_s)^2 P_{00}(k_y d)(1 - P_{00}(k_y d))}, \end{aligned} \quad (2)$$

where $\gamma = 28.02 \text{ GHz/T}$ is the electron gyromagnetic ratio and $P_{00} = 1 + [(1 - \exp(-k_y d))/k_y d]$. We note that, being $d = 100 \text{ nm}$ and $k_y d = 0.03$, Eq. 2 results very near to $\omega_{FMR} = \mu_0 \gamma \sqrt{H_0(H_0 + M_s)}$ (Fig. 1(a)). The temperature dependence of Eq. 2 derives from the saturation magnetization of YIG, M_s , which follows [41, 42, 30]

$$M_s = M_0(1 - uT^{3/2} - vT^{5/2}), \quad (3)$$

being $u = 23 \times 10^{-6} \text{ K}^{-3/2}$ and $v = 1.08 \times 10^{-7} \text{ K}^{-5/2}$ [42]. Using $\mu_0 M_0 =$

0.28 T, we can reproduce the magnetic field dependence of ω_0 in the entire temperature range (Fig. 1(a) and Fig. 2).

Higher spin wave resonances beyond ω_0 are described in the KS model as Perpendicular Standing Spin Wave (PSSW) modes [39]. The frequency of the first PSSW mode approximately follows [40]

$$\begin{aligned} \omega_1/2\pi &= \\ &= \gamma\mu_0\sqrt{\left[H_0 + \frac{2A}{M_s}\left(k_y^2 + \left(\frac{\pi}{d}\right)^2\right)\right]\left[H_0 + \frac{2A}{M_s}\left(k_y^2 + \left(\frac{\pi}{d}\right)^2\right) + M_s + H_0\left(\frac{Ms/H_0}{\pi/d}\right)^2 k_y^2\right]}, \end{aligned} \quad (4)$$

where A is the exchange constant of the YIG film. The experimental spectra in Figs. 1 and 2 can be reproduced by using $A = 5.2$ pJ/m at 30 K and $A = 5.5$ pJ/m at 10 K.

3. Coupling between magnetic film and resonator

The 100 nm thick YIG film was subsequently placed on top of the YBCO resonator to test the coupling between their modes. Transmission spectra were acquired between 10 K and 85 K with the film in contact with the resonator. Fig. 3 shows the formation of two polaritonic branches, indicating hybridization between the magnon and photon modes. At low temperature, the splitting of approximately 460 MHz corresponds to the collective coupling $g \approx 230$ MHz. As the temperature increases up to the critical temperature of YBCO, panels (a-f) show a progressive lowering of the resonator frequency (ω_c) along with a decrease in polariton splitting.

In order to extract meaningful parameters from the experimental spectra and compare them with previous results, we follow the analysis reported in [30]. The upper (Ω_+) and lower (Ω_-) polaritons can be described as the effect of the coupling between the resonator and a single magnetic mode (ω_b). Their evolution follows [8]

$$\Omega_{\pm} = \frac{1}{\sqrt{2}}\sqrt{\omega_c^2 + \omega_b^2 \pm \sqrt{(\omega_c^2 - \omega_b^2)^2 + 16\omega_c\omega_b g^2}}, \quad (5)$$

where ω_b is correlated to both magnetic field and temperature assuming that

$$\omega_b = \omega_0 + \delta_{sc}, \quad (6)$$

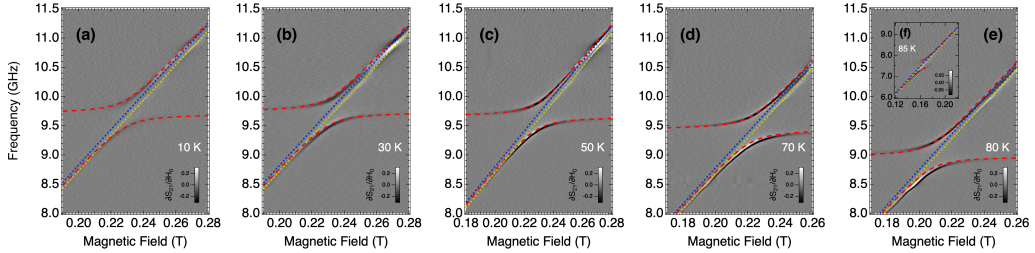


Figure 3: Transmission ($\partial S_{21} / \partial H_0$) spectra acquired at different temperatures. The YIG film is positioned in contact with the resonator and the incident microwave power is -15 dBm. For comparison, spectra taken in the same conditions with the GGG face of the sample located above the resonator do not show any resonant mode. The calculated polaritonic modes Ω_{\pm} are represented by red dashed lines; blue and yellow dashed lines show ω_0 and ω_b , respectively.

where ω_0 the frequency of the lowest YIG mode (Eq. 2) and δ_{sc} a temperature-dependent change. The latter can be quantified by self-consistently including the spin-wave induced Meissner currents in the Landau-Lifshitz-Gilbert equation, to obtain [21]

$$\delta_{sc} \approx \gamma \mu_0 M_s k_y dr \frac{1 - e^{-\frac{2t}{\lambda_L}}}{(k_y \lambda_L + 1)^2 - (k_y \lambda_L - 1)^2 e^{-\frac{2t}{\lambda_L}}}, \quad (7)$$

where t is the thickness of the YBCO film and r is a dimensionless geometrical factor associated with the YIG thickness and spin-wave ellipticity. λ_L is the penetration depth of YBCO, which in the simplest two-fluid binomial approximation reads [43]

$$\lambda_L = \frac{\lambda_L(0)}{\sqrt{1 - \left(\frac{T}{T_c}\right)^p}}, \quad (8)$$

where T_c is the critical temperature, $\lambda_L(0)$, is the London penetration length in the zero temperature limit, and $p = 4/3$ for d-wave superconductors [43, 44, 45].

By means of Eq. 5 we have fitted the evolution of polaritons in Fig. 3. The frequency of the resonator, $\omega_c(T)$, is used at each temperature as a free parameter; ω_b has been calculated using Eq. 7, where $r = 0.45$ and the penetration depth has been derived from Eq. 8 with $T_c = 86.1$ K and

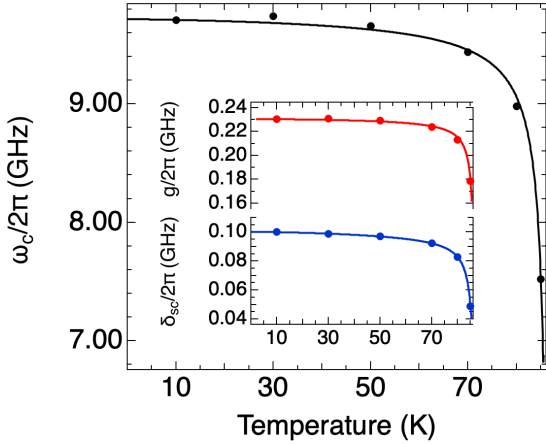


Figure 4: Frequency of the resonator extracted from transmission maps acquired at different temperatures (circles). The solid line shows the fit with Eq. 9. Inset. Coupling strength and frequency shift calculated using, respectively, the resonator frequencies (circles) and Eq. 9 (solid lines).

$\lambda_L(0) = 97$ nm. The latter parameters are obtained from the fit of $\omega_c(T)$ (Fig. 4) using [45]

$$\omega_c \approx \omega_c(0) \sqrt{\frac{L[\lambda_L(T_0)]}{L[\lambda_L(T)]}}, \quad (9)$$

being $L[\lambda_L(T)]$ the temperature-dependent inductance and $\omega_c(0) = 9.7$ GHz at $T_0 = 10$ K. Finally, the collective coupling $g = g_s \sqrt{2s_{\text{Fe}} N_s}$, where $s_{\text{Fe}} = 5/2$ is the single-ion spin of Fe^{3+} , is calculated assuming that the number of spins is $N_s = 1.49 \times 10^{13}$ in the entire temperature range. The temperature dependence of g derives, through $\omega_c(T)$, from the spin-photon coupling

$$g_s \approx \frac{\mu_0 \omega_c}{4w} \sqrt{\frac{h}{Z_0}}, \quad (10)$$

where b_{vac} is the vacuum magnetic field of the resonator and $Z_0 = 58 \Omega$ is the nominal impedance of the CPW line [30].

In summary, Fig. 4 shows the temperature evolution of the parameters that describe the experimental data. From the fitted values of $\omega_c(T)$ and using the values of $\delta_{sc}(T)$ and $g(T)$ calculated using $r = 0.45$ and $N_s = 1.49 \times 10^{13}$, we can reproduce the evolution of the polaritonic spectrum in the 10-85 K range (Fig. 3).

4. Discussion

Data acquired at low temperature using the YBCO broadband line (Fig. 1(b) and Fig. 2) evidence the presence of two magnetic modes having frequencies ω_0 and ω_1 . Their evolution as a function of magnetic field and temperature has been analyzed using the KS model and taking into account the saturation magnetization (M_s) and exchange constant (A). The values found for such parameters (Sect. 2) are in line with those reported in the literature [42, 46]. However, because the magnetic film is in contact with the surface of the superconductor, additional effects emerge due to their interplay [30] as evidenced by the comparison of transmission spectra taken at different temperatures.

The evolution of broadband maps (Fig. 2) shows that ω_1 becomes visible only at $T \leq 30$ K. The saturation magnetization and exchange constant of YIG have a weak temperature dependence in this range; by contrast, the characteristics of the YBCO film are strongly temperature dependent. In particular, the penetration depth decreases at low T , where the microwave field becomes more efficiently confined to the surface of the transmission line. In these conditions, similar to [8, 30], we note that the transmission line becomes more sensitive to spin wave modes having a short decay distance of the stray field, such as for high wavenumbers [38, 47].

The linewidths extracted from the broadband spectra in Fig. 1(c) show values larger than what is typically reported for YIG/GGG films. Losses in YIG/GGG films have been widely investigated as a function of experimental parameters such as temperature, film thickness, and wavenumber [48, 49, 50]. At room temperature, FMR resonances show linewidths well below 1 MHz; at low temperature the broadening of spin wave modes has been attributed to effects like dipolar coupling to the partially magnetized GGG substrate and relaxation of rare earth ions, resulting in linewidths between 1 and 30 MHz. Moreover, studies of magnetic losses in YIG films having conductive electrodes deposited on top have shown increased values of linewidth [51, 52, 53]. In our case, the wide linewidths in Fig. 1(c) can be attributed to the presence of the superconductor. We just mention that, due to Meissner screening and nonperfect parallelism of the film surface with respect to magnetic field, we expect field inhomogeneity at the superconductor-magnetic film interface.

Further evidence of the interplay between magnetic and superconducting layers emerges in transmission spectra acquired using the superconducting

resonator. In the first place, we note that ω_1 is not visible in Fig. 3, therefore, we can rule out the effects of higher modes observed with three-dimensional cavities [54]. Following the results obtained with 5- μm -thick YIG films [30], in Sect. 3 we have assumed that ω_b is derived by the shift of the lowest YIG mode, ω_0 (Eq. 6), as quantified by Eq. 7. In particular, the latter predicts that δ_{sc} is proportional to the thickness of the YIG film (d): the maximum value of δ_{sc} obtained in Ref. [30] for $d = 5 \mu\text{m}$ exceeds 1 GHz whereas in the present case ($d = 100 \text{ nm}$) δ_{sc} drops to 0.1 GHz (Fig. 4). However, we notice that the geometrical factor r used to fit the spectra is different in the two cases. These parameters well reproduce the evolution of the transmission data in Fig. 3. The absence of a noticeable frequency shift in the broadband spectra (Fig. 2) could be related to the relatively wide linewidth of ω_0 (Fig. 1(c)).

It is interesting to compare the coupling strength values (g) obtained with YIG films having different thicknesses, though similar lateral dimensions, and obtained using YBCO resonators having the same geometry. The maximum coupling strength derived from the spectra in Fig. 3 is 0.23 GHz while the coupling obtained with a 5- μm -thick YIG film is around 1.1 GHz [30]. We first note that the ratio between the thicknesses is 50 while the coupling strength achieved with the thicker film is 5 times higher; considering that $g \propto \sqrt{N_s}$, where N_s is the product of the YIG spin density and the intersection of the resonator and YIG film volumes, we infer that the coupling strength does not scale as the square root of the thickness of the latter. In addition, the distribution of the microwave field obtained from the results of electromagnetic simulations, at least for the bare CPW resonator, stretches well above a few microns from the resonator surface [8]. If the magnetic system was paramagnetic or if the mode had uniform precession of the magnetization, all the spins, positioned in a 100-nm-thick layer above the surface of the resonator and located sufficiently near to the central conductor, were uniformly excited by the microwave field. However, the coupling strength estimated using the spin density of the YIG film results much higher than what derived from the experiment; this indicates that in the latter case the precession of the spins is nonuniform, *i.e.* the spin texture of the hybrid mode is more complex. Thus, while the spin-photon coupling is determined by the vacuum magnetic field of the resonator (Eq. 10), the collective coupling, as suggested by simple calculations, is related to the specific way in which the electromagnetic and spin waves combine in the magnet/superconductor bilayer to shape the hybrid mode.

5. Conclusions

In conclusion, we have studied the microwave response of nonconductive 100-nm-thick YIG films positioned on top of a YBCO superconducting layer. Transmission spectra were acquired at different temperatures either by using a broadband CPW line or a CPW resonator. In the former case, experimental data have been essentially reproduced using well-known formulae and physical quantities describing the spin-wave excitation spectrum of the YIG film. In the latter case, the coupling extracted from the splitting of magnon-photon polaritons amounts to 230 MHz. The evolution of the polaritonic spectrum at different temperatures can be attributed to the effects of the penetration depth of the YBCO superconductor. The comparison with the results obtained with a thicker YIG film suggests a non-trivial role of both system geometry and material parameters in determining the collective coupling strength.

Acknowledgments

This work was partially supported by the project SMILE-SQUIP funded by the Italian NQSTI - National Quantum Science and Technology Institute code PE0000 0023 and by the U.S. Office of Naval Research Award No. N62909-23-1-2079. A.G. acknowledges financial support from PNRR MUR project ECS_00000033_ECOSISTER.

References

- [1] D. Lachance-Quirion, Y. Tabuchi, S. Ishino, A. Noguchi, T. Ishikawa, R. Yamazaki, Y. Nakamura, [Resolving quanta of collective spin excitations in a millimeter-sized ferromagnet](#), *Science Advances* 3 (7) (2017) e1603150. doi:[10.1126/sciadv.1603150](https://doi.org/10.1126/sciadv.1603150).
URL <https://www.science.org/doi/abs/10.1126/sciadv.1603150>
- [2] H. Yuan, Y. Cao, A. Kamra, R. A. Duine, P. Yan, [Quantum magnonics: When magnon spintronics meets quantum information science](#), *Physics Reports* 965 (2022) 1–74, quantum magnonics: When magnon spintronics meets quantum information science. doi:<https://doi.org/10.1016/j.physrep.2022.03.002>.
URL <https://www.sciencedirect.com/science/article/pii/S0370157322000977>

- [3] Y.-P. Wang, G.-Q. Zhang, D. Zhang, T.-F. Li, C.-M. Hu, J. Q. You, **Bistability of cavity magnon polaritons**, Phys. Rev. Lett. 120 (2018) 057202. doi:[10.1103/PhysRevLett.120.057202](https://doi.org/10.1103/PhysRevLett.120.057202).
URL <https://link.aps.org/doi/10.1103/PhysRevLett.120.057202>

- [4] O. Lee, K. Yamamoto, M. Umeda, C. W. Zollitsch, M. Elyasi, T. Kikkawa, E. Saitoh, G. E. W. Bauer, H. Kurebayashi, **Nonlinear magnon polaritons**, Phys. Rev. Lett. 130 (2023) 046703. doi:[10.1103/PhysRevLett.130.046703](https://doi.org/10.1103/PhysRevLett.130.046703).
URL <https://link.aps.org/doi/10.1103/PhysRevLett.130.046703>

- [5] M.-X. Bi, H. Fan, X.-H. Yan, Y.-C. Lai, **Folding state within a hysteresis loop: Hidden multistability in nonlinear physical systems**, Phys. Rev. Lett. 132 (2024) 137201. doi:[10.1103/PhysRevLett.132.137201](https://doi.org/10.1103/PhysRevLett.132.137201).
URL <https://link.aps.org/doi/10.1103/PhysRevLett.132.137201>

- [6] J. Bourhill, N. Kostylev, M. Goryachev, D. L. Creedon, M. E. Tobar, **Ultrahigh cooperativity interactions between magnons and resonant photons in a yig sphere**, Phys. Rev. B 93 (2016) 144420. doi:[10.1103/PhysRevB.93.144420](https://doi.org/10.1103/PhysRevB.93.144420).
URL <https://link.aps.org/doi/10.1103/PhysRevB.93.144420>

- [7] I. A. Golovchanskiy, N. N. Abramov, V. S. Stolyarov, A. A. Golubov, M. Y. Kupriyanov, V. V. Ryazanov, A. V. Ustinov, **Approaching deep-strong on-chip photon-to-magnon coupling**, Phys. Rev. Applied 16 (2021) 034029. doi:[10.1103/PhysRevApplied.16.034029](https://doi.org/10.1103/PhysRevApplied.16.034029).
URL <https://link.aps.org/doi/10.1103/PhysRevApplied.16.034029>

- [8] A. Gherri, C. Bonizzoni, M. Maksutoglu, A. Mercurio, O. Di Stefano, S. Savasta, M. Affronte, **Ultrastrong magnon-photon coupling achieved by magnetic films in contact with superconducting resonators**, Phys. Rev. Appl. 20 (2023) 024039. doi:[10.1103/PhysRevApplied.20.024039](https://doi.org/10.1103/PhysRevApplied.20.024039).
URL <https://link.aps.org/doi/10.1103/PhysRevApplied.20.024039>

- [9] D. Zhang, X.-Q. Luo, Y.-P. Wang, T.-F. Li, J. Q. You, Observation of the exceptional point in cavity magnon-polaritons, *Nature Communications* 8 (1) (2017) 1368.
- [10] T. Yu, J. Zou, B. Zeng, J. Rao, K. Xia, [Non-hermitian topological magnonics](#), *Physics Reports* 1062 (2024) 1–86, non-Hermitian topological magnonics. [doi:<https://doi.org/10.1016/j.physrep.2024.01.006>](https://doi.org/10.1016/j.physrep.2024.01.006).
URL <https://www.sciencedirect.com/science/article/pii/S0370157324000309>
- [11] J. Xu, C. Zhong, X. Han, D. Jin, L. Jiang, X. Zhang, [Floquet cavity electromagnonics](#), *Phys. Rev. Lett.* 125 (2020) 237201. [doi:\[10.1103/PhysRevLett.125.237201\]\(https://doi.org/10.1103/PhysRevLett.125.237201\)](https://doi.org/10.1103/PhysRevLett.125.237201).
URL <https://link.aps.org/doi/10.1103/PhysRevLett.125.237201>
- [12] J. W. Rao, B. Yao, C. Y. Wang, C. Zhang, T. Yu, W. Lu, [Unveiling a pump-induced magnon mode via its strong interaction with walker modes](#), *Phys. Rev. Lett.* 130 (2023) 046705. [doi:\[10.1103/PhysRevLett.130.046705\]\(https://doi.org/10.1103/PhysRevLett.130.046705\)](https://doi.org/10.1103/PhysRevLett.130.046705).
URL <https://link.aps.org/doi/10.1103/PhysRevLett.130.046705>
- [13] D. Lachance-Quirion, Y. Tabuchi, A. Gloppe, K. Usami, Y. Nakamura, [Hybrid quantum systems based on magnonics](#), *Appl. Phys. Express* 12 (2019).
- [14] Y. Li, W. Zhang, V. Tyberkevych, W.-K. Kwok, A. Hoffmann, V. Novosad, [Hybrid magnonics: Physics, circuits, and applications for coherent information processing](#), *Journal of Applied Physics* 128 (13) (2020) 130902. [doi:\[10.1063/5.0020277\]\(https://doi.org/10.1063/5.0020277\)](https://doi.org/10.1063/5.0020277).
URL <https://doi.org/10.1063/5.0020277>
- [15] P. Pirro, V. I. Vasyuchka, A. A. Serga, B. Hillebrands, [Advances in coherent magnonics](#), *Nature Reviews Materials* 6 (12) (2021) 1114–1135.
URL <https://doi.org/10.1038/s41578-021-00332-w>
- [16] B. Zare Rameshti, S. Viola Kusminskiy, J. A. Haigh, K. Usami, D. Lachance-Quirion, Y. Nakamura, C.-M. Hu, H. X. Tang, G. E.

- Bauer, Y. M. Blanter, [Cavity magnonics](#), Physics Reports 979 (2022) 1–61.
URL <https://www.sciencedirect.com/science/article/pii/S0370157322002460>
- [17] A. V. Chumak, P. Kabos, M. Wu, C. Abert, C. Adelmann, A. O. Adeyeye, J. Åkerman, F. G. Aliev, A. Anane, A. Awad, C. H. Back, A. Barman, G. E. W. Bauer, M. Becherer, E. N. Beginin, V. A. S. V. Bittencourt, Y. M. Blanter, P. Bortolotti, I. Boventer, D. A. Bozhko, S. A. Bunyaev, J. J. Carmiggelt, R. R. Cheenikundil, F. Ciubotaru, S. Cotofana, G. Csaba, O. V. Dobrovolskiy, C. Dubs, M. Elyasi, K. G. Fripp, H. Fulara, I. A. Golovchanskiy, C. Gonzalez-Ballester, P. Graczyk, D. Grundler, P. Gruszecki, G. Gubbiotti, K. Guslienko, A. Haldar, S. Hamdioui, R. Hertel, B. Hillebrands, T. Hioki, A. Houshang, C.-M. Hu, H. Huebl, M. Huth, E. Iacobca, M. B. Jungfleisch, G. N. Kakazei, A. Khitun, R. Khymyn, T. Kikkawa, M. Kläui, O. Klein, J. W. Kłos, S. Knauer, S. Koraltan, M. Kostylev, M. Krawczyk, I. N. Krivorotov, V. V. Kruglyak, D. Lachance-Quirion, S. Ladak, R. Lebrun, Y. Li, M. Lindner, R. Macêdo, S. Mayr, G. A. Melkov, S. Miesczak, Y. Nakamura, H. T. Nembach, A. A. Nikitin, S. A. Nikitov, V. Novosad, J. A. Otalora, Y. Otani, A. Papp, B. Pigeau, P. Pirro, W. Porod, F. Porrati, H. Qin, B. Rana, T. Reimann, F. Riente, O. Romero-Isart, A. Ross, A. V. Sadovnikov, A. R. Safin, E. Saitoh, G. Schmidt, H. Schultheiss, K. Schultheiss, A. A. Serga, S. Sharma, J. M. Shaw, D. Suess, O. Surzhenko, K. Szulc, T. Taniguchi, M. Urbanek, K. Usami, A. B. Ustinov, T. van der Sar, S. van Dijken, V. I. Vasyuchka, R. Verba, S. V. Kusminskiy, Q. Wang, M. Weides, M. Weiler, S. Wintz, S. P. Wolski, X. Zhang, Advances in magnetics roadmap on spin-wave computing, IEEE Transactions on Magnetics 58 (6) (2022) 1–72. [doi:10.1109/TMAG.2022.3149664](#).
- [18] X. Han, H. Wu, T. Zhang, [Magnonics: Materials, physics, and devices](#), Applied Physics Letters 125 (2) (2024) 020501. [doi:10.1063/5.0216094](#).
URL <https://doi.org/10.1063/5.0216094>
- [19] O. V. Dobrovolskiy, R. Sachser, T. Brächer, T. Böttcher, V. V. Kruglyak, R. V. Vovk, V. A. Shklovskij, M. Huth, B. Hillebrands, A. V. Chumak, [Magnon–fluxon interaction in a ferromagnet/superconductor](#)

- heterostructure, Nature Physics 15 (5) (2019) 477–482. doi:10.1038/s41567-019-0428-5.
URL <https://doi.org/10.1038/s41567-019-0428-5>
- [20] I. A. Golovchanskiy, N. N. Abramov, V. S. Stolyarov, P. S. Dzhumaev, O. V. Emelyanova, A. A. Golubov, V. V. Ryazanov, A. V. Ustinov, Ferromagnet/superconductor hybrid magnonic metamaterials, Advanced Science 6 (16) (2019) 1900435. doi:<https://doi.org/10.1002/advs.201900435>.
URL <https://advanced.onlinelibrary.wiley.com/doi/abs/10.1002/advs.201900435>
- [21] M. Borst, P. H. Vree, A. Lowther, A. Teepe, S. Kurdi, I. Bertelli, B. G. Simon, Y. M. Blanter, T. van der Sar, Observation and control of hybrid spin-wave–meissner-current transport modes, Science 382 (6669) (2023) 430–434. doi:10.1126/science.adj7576.
URL <https://www.science.org/doi/abs/10.1126/science.adj7576>
- [22] C. G. L. Böttcher, N. R. Poniatowski, A. Grankin, M. E. Wesson, Z. Yan, U. Vool, V. M. Galitski, A. Yacoby, Circuit quantum electrodynamics detection of induced two-fold anisotropic pairing in a hybrid superconductor–ferromagnet bilayer, Nature Physics (2024). doi:10.1038/s41567-024-02613-x.
URL <https://doi.org/10.1038/s41567-024-02613-x>
- [23] H. Huebl, C. W. Zollitsch, J. Lotze, F. Hocke, M. Greifenstein, A. Marx, R. Gross, S. T. B. Goennenwein, High cooperativity in coupled microwave resonator ferrimagnetic insulator hybrids, Phys. Rev. Lett. 111 (2013) 127003. doi:10.1103/PhysRevLett.111.127003.
URL <https://link.aps.org/doi/10.1103/PhysRevLett.111.127003>
- [24] R. G. E. Morris, A. F. van Loo, S. Kosen, A. D. Karenowska, Strong coupling of magnons in a yig sphere to photons in a planar superconducting resonator in the quantum limit, Scientific Reports 7 (1) (2017) 11511. doi:10.1038/s41598-017-11835-4.
URL <https://doi.org/10.1038/s41598-017-11835-4>

- [25] J. T. Hou, L. Liu, [Strong coupling between microwave photons and nanomagnet magnons](#), Phys. Rev. Lett. 123 (2019) 107702.
 URL <https://link.aps.org/doi/10.1103/PhysRevLett.123.107702>
- [26] Y. Li, T. Polakovic, Y.-L. Wang, J. Xu, S. Lendinez, Z. Zhang, J. Ding, T. Khaire, H. Saglam, R. Divan, J. Pearson, W.-K. Kwok, Z. Xiao, V. Novosad, A. Hoffmann, W. Zhang, [Strong coupling between magnons and microwave photons in on-chip ferromagnet-superconductor thin-film devices](#), Phys. Rev. Lett. 123 (2019) 107701.
`doi:10.1103/PhysRevLett.123.107701.`
 URL <https://link.aps.org/doi/10.1103/PhysRevLett.123.107701>
- [27] I. A. Golovchanskiy, N. N. Abramov, V. S. Stolyarov, V. V. Ryazanov, A. A. Golubov, A. V. Ustinov, [Modified dispersion law for spin waves coupled to a superconductor](#), Journal of Applied Physics 124 (23) (2018) 233903. `doi:10.1063/1.5077086.`
 URL <https://doi.org/10.1063/1.5077086>
- [28] I. A. Golovchanskiy, N. N. Abramov, V. S. Stolyarov, M. Weides, V. V. Ryazanov, A. A. Golubov, A. V. Ustinov, M. Y. Kupriyanov, [Ultra-strong photon-to-magnon coupling in multilayered heterostructures involving superconducting coherence via ferromagnetic layers](#), Science Advances 7 (25) (2021) eabe8638. `doi:10.1126/sciadv.abe8638.`
 URL <https://www.science.org/doi/abs/10.1126/sciadv.abe8638>
- [29] I. A. Golovchanskiy, N. N. Abramov, O. V. Emelyanova, I. V. Shchetinin, V. V. Ryazanov, A. A. Golubov, V. S. Stolyarov, [Magnetization dynamics in proximity-coupled superconductor-ferromagnet-superconductor multilayers. ii. thickness dependence of the superconducting torque](#), Phys. Rev. Appl. 19 (2023) 034025. `doi:10.1103/PhysRevApplied.19.034025.`
 URL <https://link.aps.org/doi/10.1103/PhysRevApplied.19.034025>
- [30] A. Gherri, C. Bonizzoni, M. Maksutoglu, M. Affronte, [Interplay between magnetism and superconductivity in a hybrid magnon-photon bilayer system](#), Phys. Rev. Appl. 22 (2024) 034004.

- [doi:10.1103/PhysRevApplied.22.034004](https://doi.org/10.1103/PhysRevApplied.22.034004).
URL <https://link.aps.org/doi/10.1103/PhysRevApplied.22.034004>
- [31] D. Xu, X.-K. Gu, H.-K. Li, Y.-C. Weng, Y.-P. Wang, J. Li, H. Wang, S.-Y. Zhu, J. Q. You, [Quantum control of a single magnon in a macroscopic spin system](#), Phys. Rev. Lett. 130 (2023) 193603. [doi:10.1103/PhysRevLett.130.193603](https://doi.org/10.1103/PhysRevLett.130.193603).
URL <https://link.aps.org/doi/10.1103/PhysRevLett.130.193603>
- [32] A. Ghirri, C. Bonizzoni, D. Gerace, S. Sanna, A. Cassinese, M. Affronte, [Yba2cu3o7 microwave resonators for strong collective coupling with spin ensembles](#), Applied Physics Letters 106 (18) (2015) 184101. [doi:10.1063/1.4920930](https://doi.org/10.1063/1.4920930).
URL <https://doi.org/10.1063/1.4920930>
- [33] C. Bonizzoni, A. Ghirri, F. Santanni, M. Atzori, L. Sorace, R. Sessoli, M. Affronte, [Storage and retrieval of microwave pulses with molecular spin ensembles](#), npj Quantum Information 6 (1) (2020) 68. [doi:10.1038/s41534-020-00296-9](https://doi.org/10.1038/s41534-020-00296-9).
URL <https://doi.org/10.1038/s41534-020-00296-9>
- [34] C. Bonizzoni, M. Maksutoglu, A. Ghirri, J. van Tol, B. Rameev, M. Affronte, [Coupling sub-nanoliter bdpa organic radical spin ensembles with ybco inverse anapole resonators](#), Applied Magnetic Resonance 54 (1) (2023) 143–164. [doi:10.1007/s00723-022-01505-8](https://doi.org/10.1007/s00723-022-01505-8).
URL <https://doi.org/10.1007/s00723-022-01505-8>
- [35] Z. Velluire-Pellat, E. Maréchal, N. Moulouguet, G. Saïz, G. C. Ménard, S. Kozlov, F. Couëdo, P. Amari, C. Medous, J. Paris, R. Hostein, J. Lesueur, C. Feuillet-Palma, N. Bergeal, [Hybrid quantum systems with high-t\\$c\\$superconducting resonators](#), Scientific Reports 13 (1) (2023) 14366.
URL <https://doi.org/10.1038/s41598-023-41472-z>
- [36] C. Bonizzoni, A. Ghirri, F. Santanni, M. Affronte, [Quantum sensing of magnetic fields with molecular spins](#), npj Quantum Information 10 (1) (2024) 41. [doi:10.1038/s41534-024-00838-5](https://doi.org/10.1038/s41534-024-00838-5).
URL <https://doi.org/10.1038/s41534-024-00838-5>

- [37] C. P. Poole, H. A. Farach, [Lineshapes in electron spin resonance](#), Bull. Magn. Reson. 1 (1979) 162–194.
URL https://ismar.org/wp-content/uploads/2021/09/BMR_01_162-194_1979.pdf
- [38] I. S. Maksymov, M. Kostylev, [Broadband stripline ferromagnetic resonance spectroscopy of ferromagnetic films, multilayers and nanostructures](#), Physica E: Low-dimensional Systems and Nanostructures 69 (2015) 253–293. doi:<https://doi.org/10.1016/j.physe.2014.12.027>.
URL <https://www.sciencedirect.com/science/article/pii/S1386947714004664>
- [39] B. A. Kalinikos, A. N. Slavin, [Theory of dipole-exchange spin wave spectrum for ferromagnetic films with mixed exchange boundary conditions](#), Journal of Physics C: Solid State Physics 19 (35) (1986) 7013. doi:[10.1088/0022-3719/19/35/014](https://doi.org/10.1088/0022-3719/19/35/014).
URL <https://dx.doi.org/10.1088/0022-3719/19/35/014>
- [40] S. O. Demokritov, A. N. Slavin, Spin Waves, Springer International Publishing, Cham, 2021, pp. 281–346. doi:[10.1007/978-3-030-63210-6_6](https://doi.org/10.1007/978-3-030-63210-6_6).
- [41] J. Solt, Irvin H., [Temperature Dependence of YIG Magnetization](#), Journal of Applied Physics 33 (3) (2004) 1189–1191. doi:[10.1063/1.1728651](https://doi.org/10.1063/1.1728651).
URL <https://doi.org/10.1063/1.1728651>
- [42] H. Maier-Flaig, S. Klingler, C. Dubs, O. Surzhenko, R. Gross, M. Weiler, H. Huebl, S. T. B. Goennenwein, [Temperature-dependent magnetic damping of yttrium iron garnet spheres](#), Phys. Rev. B 95 (2017) 214423. doi:[10.1103/PhysRevB.95.214423](https://doi.org/10.1103/PhysRevB.95.214423).
URL <https://link.aps.org/doi/10.1103/PhysRevB.95.214423>
- [43] R. Prozorov, R. W. Giannetta, [Magnetic penetration depth in unconventional superconductors](#), Superconductor Science and Technology 19 (8) (2006) R41.
URL <https://dx.doi.org/10.1088/0953-2048/19/8/R01>

- [44] O. Vendik, I. Vendik, D. Kaparkov, Empirical model of the microwave properties of high-temperature superconductors, *IEEE Transactions on Microwave Theory and Techniques* 46 (5) (1998) 469–478. [doi:10.1109/22.668643](https://doi.org/10.1109/22.668643).
- [45] G. Ghigo, D. Botta, A. Chiodoni, R. Gerbaldo, L. Gozzelino, F. Laviano, B. Minetti, E. Mezzetti, D. Andreone, [Microwave dissipation in ybco coplanar resonators with uniform and non-uniform columnar defect distribution](#), *Superconductor Science and Technology* 17 (8) (2004) 977. [doi:10.1088/0953-2048/17/8/004](https://doi.org/10.1088/0953-2048/17/8/004)
URL <https://dx.doi.org/10.1088/0953-2048/17/8/004>
- [46] A. M. Zyuzin, A. G. Bazhanov, [Temperature dependence of the exchange interaction constant in iron garnet films](#), *Journal of Experimental and Theoretical Physics Letters* 63 (7) (1996) 555–559. [doi:10.1134/1.567056](https://doi.org/10.1134/1.567056).
URL <https://doi.org/10.1134/1.567056>
- [47] I. Bertelli, J. J. Carmiggelt, T. Yu, B. G. Simon, C. C. Pothoven, G. E. W. Bauer, Y. M. Blanter, J. Aarts, T. van der Sar, [Magnetic resonance imaging of spin-wave transport and interference in a magnetic insulator](#), *Science Advances* 6 (46) (2020) eabd3556. [arXiv: https://www.science.org/doi/pdf/10.1126/sciadv.abd3556](https://www.science.org/doi/pdf/10.1126/sciadv.abd3556), doi: [10.1126/sciadv.abd3556](https://doi.org/10.1126/sciadv.abd3556).
URL <https://www.science.org/doi/abs/10.1126/sciadv.abd3556>
- [48] C. Dubs, O. Surzhenko, R. Linke, A. Danilewsky, U. Bruckner, J. Dellith, [Sub-micrometer yttrium iron garnet lpe films with low ferromagnetic resonance losses](#), *Journal of Physics D: Applied Physics* 50 (20) (2017) 204005. [doi:10.1088/1361-6463/aa6b1c](https://doi.org/10.1088/1361-6463/aa6b1c).
URL <https://dx.doi.org/10.1088/1361-6463/aa6b1c>
- [49] Y. Rao, D. Zhang, H. Zhang, L. Jin, Q. Yang, Z. Zhong, M. Li, C. Hong, B. Ma, [Thickness dependence of magnetic properties in submicron yttrium iron garnet films](#), *Journal of Physics D: Applied Physics* 51 (43) (2018) 435001. [doi:10.1088/1361-6463/aade43](https://doi.org/10.1088/1361-6463/aade43).
URL <https://dx.doi.org/10.1088/1361-6463/aade43>
- [50] D. Schmoll, A. A. Voronov, R. O. Serha, D. Slobodianuk, K. O. Levchenko, C. Abert, S. Knauer, D. Suess, R. Verba, A. V. Chumak,

- Wavenumber-dependent magnetic losses in yig-ggg heterostructures at millikelvin temperatures (2024). [arXiv:2411.13414](https://arxiv.org/abs/2411.13414).
URL <https://arxiv.org/abs/2411.13414>
- [51] S. M. Rezende, R. L. Rodriguez-Suarez, M. M. Soares, L. H. Vilela-Leqo, D. Ley Dominguez, A. Azevedo, Enhanced spin pumping damping in yttrium iron garnet/pt bilayers, Applied Physics Letters 102 (1) (2013) 012402. [doi:10.1063/1.4773993](https://doi.org/10.1063/1.4773993).
URL <https://doi.org/10.1063/1.4773993>
- [52] S. A. Bunyaev, R. O. Serha, H. Y. Musiienko-Shmarova, A. J. Kreil, P. Frey, D. A. Bozhko, V. I. Vasyuchka, R. V. Verba, M. Kostylev, B. Hillebrands, G. N. Kakazei, A. A. Serga, Spin-wave relaxation by eddy currents in $y_3fe_5o_{12}$ /Pt bilayers and a way to suppress it, Phys. Rev. Appl. 14 (2020) 024094. [doi:10.1103/PhysRevApplied.14.024094](https://doi.org/10.1103/PhysRevApplied.14.024094).
URL <https://link.aps.org/doi/10.1103/PhysRevApplied.14.024094>
- [53] D. Schmoll, R. O. Serha, J. Panda, A. A. Voronov, C. Dubs, M. Urbánek, A. V. Chumak, Elimination of substrate-induced fmr linewidth broadening in the epitaxial system yig-ggg by microstructuring (2025). [arXiv:2502.02978](https://arxiv.org/abs/2502.02978).
URL <https://arxiv.org/abs/2502.02978>
- [54] Y. Cao, P. Yan, H. Huebl, S. T. B. Goennenwein, G. E. W. Bauer, Exchange magnon-polaritons in microwave cavities, Phys. Rev. B 91 (2015) 094423. [doi:10.1103/PhysRevB.91.094423](https://doi.org/10.1103/PhysRevB.91.094423).
URL <https://link.aps.org/doi/10.1103/PhysRevB.91.094423>